Geomechanics and Engineering, *Vol. 18, No. 6 (2019) 595-603*
DOI: https://doi.org/10.12989/gae.2019.18.6.595

Probabilistic analysis for face stability of tunnels in Hoek-Brown media

T.Z. Li[1,2] and X.L. Yang*[2]

[1]Department of Civil and Architecture Engineering, Changzhou Institute of Technology, Jiangsu, China
[2]School of Civil Engineering, Central South University, Hunan 410075, China

(Received February 1, 2019, Revised August 10, 2019, Accepted August 14, 2019)

Abstract. A modified model combining Kriging and Monte Carlo method (MC) is proposed for probabilistic estimation of tunnel face stability in this paper. In the model, a novel uniform design is adopted to train the Kriging, instead of the existing active learning function. It has advantage of avoiding addition of new training points iteratively, and greatly saves the computational time in model training. The kinematic approach of limit analysis is employed to define the deterministic computational model of face failure, in which the Hoek-Brown failure criterion is introduced to account for the nonlinear behaviors of rock mass. The trained Kriging is used as a surrogate model to perform MC with dramatic reduction of calls to actual limit state function. The parameters in Hoek-Brown failure criterion are considered as random variables in the analysis. The failure probability is estimated by direct MC to test the accuracy and efficiency of the proposed probabilistic model. The influences of uncertainty level, correlation relationship and distribution type of random variables are further discussed using the proposed approach. In summary, the probabilistic model is an accurate and economical alternative to perform probabilistic stability analysis of tunnel face excavated in spatially random Hoek- Brown media.

Keywords: probabilistic model; tunnel face stability; Hoek-Brown criterion; kriging; uniform design

1. Introduction

Currently, stability problem of tunnel face is one of the research focuses in geotechnical engineering. The studies in this field are traditionally performed by developing deterministic computational models to replace the complex system failure processes using numerical approaches or simulations, such as limit analysis theory, limit equilibrium method, finite element analysis and other methods (Aminpour *et al*. 2017, Nian *et al*. 2014, Soomro *et al.* 2017, Zou and Xia 2016). Those approaches are efficient and accurate in predicting critical support pressure against tunnel face.

As an important issue affecting face stability, the nonlinearity of excavation media has attracted a lot of attentions of scholars. The Hoek-Brown failure criterion was proposed to describe the nonlinear properties of rock mass. In terms of its superior performance in modelling rock failure, Hoek-Brown criterion has been widely adopted in literature. Serrano *et al.* (2016) used the modified Hoek-Brown criterion to calculate the ultimate bearing capacity of a strip foundation of an anisotropic discontinuous rock mass. Yang and Chen (2019) investigated the effect of water pressure on three-dimensional (3D) unsaturated soil slope stability. Xu and Yang (2019) studied the stability of soil slope subjected to water drawdown and presented the stability charts for practical use. In contrast, those deterministic models with a nonlinear failure criterion are more convincing in characterizing rock failure.

Another issue involved with face stability is uncertainties of rock properties. Given the inherent spatial variability of rock mass, designers in practical engineering often pay more attention to how stable the tunnel face is rather than whether it is stable. For this sake, probabilistic approaches are introduced to evaluate the face stability considering the influence of uncertainties of rock properties (Miro *et al.* 2015). Crude MC is the most straightforward and robust approach to perform probabilistic stability analysis of tunnel face, but it suffers from low computational efficiency and expensive costs. In addition, the first-order and second-order reliability methods (FORM/SORM) are also commonly used approaches which are, however, not applicable for cases with nonlinear or implicit limit state functions.

In view of previous studies, deterministic models for tunnel face or slope stability are often strongly nonlinear and implicit which causes great trouble in performing probabilistic analysis with traditional reliability methods (Paternesi *et al.* 2017). To address this problem, several advanced probabilistic approaches are proposed. The response surface method (RSM) is commonly adopted to fit the implicit limit state function by assuming a closed-form polynomial in advance. But it is less efficient in those cases whose actual limit state functions are multimodal functions with several peaks and troughs. Recently, a new strategy combining metamodels and MC to construct an efficient approximation model prevails in engineering reliability analysis. Echard *et al.* (2011) proposed an active learning reliability method combining Kriging and MC, which was proved to be accurate enough with a minor number of calls to the deterministic model. Pan and Dias (2017) developed

*Corresponding author, Professor
E-mail: csuyang@aliyun.com

http://www.techno-press.org/?journal=gae&subpage=7
ISSN: 2005-307X (Print), 2092-6219 (Online)

an efficient reliability method by taking advantage of the adaptive support vector machine (SVM) and MC. Four representative examples were referred to as validations. These models were trained with active learning function by adding the new points in the training data one by one until the requirement was satisfied.

Another efficient way for model training is called as uniform design which uniformly chooses the training points in the design space without addition of new training points but can get a similar computational accuracy with that obtained by those active learning approaches. Jiang *et al.* (2015) proposed an efficient method of uniform design for SVM training to fit the structural failure function. The advanced structural analysis tool (e.g., Finite Element Analysis) was used to solve each pair of loads under the principle of approximation to the limit load and distribution on its two sides. These metamodel-based probabilistic approaches show great superiority and broad applicability in failure probability calculation of engineering structures.

This paper is devoted to a probabilistic model for stability analysis of 3D tunnel face excavated in spatially random Hoek-Brown rock mass. mi, GSI, D and σ_c are regarded as random variables to investigate the influence of uncertainties of Hoek-Brown parameters on face failure. A novel uniform design is proposed to train the Kriging by designing a series of sampling points that are uniformly distributed in the space of random variables. Unlike the existing active learning function, the uniform design does not require to adding new points to training data iteratively and subsequently can improve the model training efficiency without sacrificing estimation accuracy. The random data generated by MC are evaluated using the trained Kriging with small number of calls to the actual limit state function. The proposed probabilistic model is proved to be accurate and efficient in failure probability estimation of tunnel face considering nonlinear Hoek-Brown criterion.

2. Deterministic computational model

2.1 Nonlinear Hoek-Brown failure criterion

The linear Mohr-Coulomb failure criterion has been widely used in engineering due to its straightforward statement of stress-strain relationship of geotechnical materials (Li and Yang 2019a, e, f). However, researchers find that almost all rock and soil materials exhibit a nonlinear behavior in laboratory tests. The internal friction angle is not constant but reduces with the increase of confining pressure, eventually forming a curved Mohr's envelope. These findings necessitate the proposal of nonlinear failure criteria. To fulfill this demand, Hoek-Brown criterion was proposed in an attempt to provide a more reliable way to study rock failure (Hoek *et al.* 2002). It is written as

$$\sigma_1 = \sigma_3 + \sigma_c\left(m_b\sigma_3 / \sigma_c + s\right)^n \tag{1}$$

The expressions of mb, s and n are

$$m = m_i \exp\left(\frac{GSI-100}{28-14D}\right) \tag{2}$$

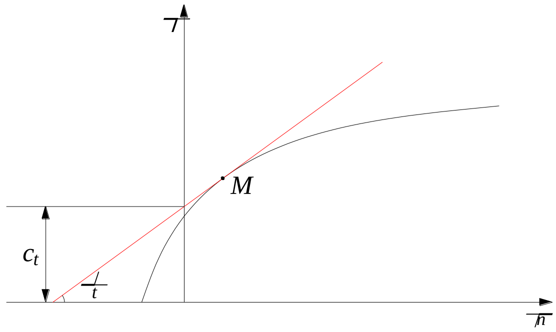

Fig. 1 Tangential line to the Hoek-Brown strength curve

$$s = \exp\left(\frac{GSI-100}{9-3D}\right) \tag{3}$$

$$n = \frac{1}{2} + \frac{1}{6}\left[\exp\left(-\frac{GSI}{15}\right) - \exp\left(-\frac{20}{3}\right)\right] \tag{4}$$

where σ1 and σ3 are respectively the major and minor principal stresses at failure; σc is the uniaxial compressive stress of the rock at failure; GSI is the geological strength index, which represents the integrity of the rock mass; D is the disturbance coefficient which varies from 0 for undisturbed rock mass to 1.0 for heavily disturbed one and mi represents the rock material constant determined by rock type.

2.2 Generalized tangential technique

In order to facilitate the usage of Hoek-Brown failure criterion in Mohr-Coulomb failure criterion-based geotechnical software, Hoek and Brown (Hoek *et al.* 2002) gave the equivalent cohesion and internal friction angle by fitting an average linear relationship to the curve generated by Eq. (1). Obviously, results obtained by this method is not the real upper bound solutions due to the intersection with Hoek-Brown strength curve. To overcome this problem, An effective approach is to simplify the nonlinear criterion into a linear one. Based on this approach, the generalized tangential technique (Li and Yang 2019c, d). The method was extended to evaluate stability problem with nonlinear failure criterion and limit analysis (Qin and Chian 2017, Ausilion and Zimmaro 2017, Li and Yang 2019b). As shown in Fig. 1, the tangential line can be expressed as

$$\tau = c_t + \sigma_n \tan\varphi_t \tag{5}$$

where c_t, φ_t are respectively the intercept and slope angle of tangential line. According to the tangential technique, ct can be expressed as a function of φt in combination of nonlinear Hoek-Brown criterion.

$$c_t = \frac{\sigma_c\cos\varphi_t}{2}\left[\frac{mn(1-\sin\varphi_t)}{2\sin\varphi_t}\right]^{\frac{n}{1-n}} - \frac{\sigma_c\tan\varphi_t}{m}\left(1+\frac{\sin\varphi_t}{n}\right)\left[\frac{mn(1-\sin\varphi_t)}{2\sin\varphi_t}\right]^{\frac{1}{1-n}} + \frac{\sigma_c s\tan\varphi_t}{m} \tag{6}$$

Scholars directly used ct, φt instead of cohesion and internal friction angle to formulate external work rate and internal energy dissipation based on upper bound theorem of limit analysis. Due to the convex failure surface of Hoek-

Brown criterion, the limit load solved by the tangential technique is equal to or larger than that by actual failure surface, which ensures an upper bound solution.

2.3 Limit analysis of tunnel face stability

Limit analysis is widely used in engineering (Yang and Chen 2019a, b, Zhang and Yang 2019a, b). In this section, it is performed routinely to construct the deterministic computational model of tunnel face failure. As shown in Fig. 2, a 3D rotational failure mechanism of tunnel face is presented according to Michalowski and Drescher (2009). The profile of the curved rigid cone is fundamentally composed of two crossed and same-centered logspiral curves which respectively start from the tunnel roof and tunnel invert and outline the upper and lower boundaries. C, d respectively denote the buried depth and diameter of tunnel. ω is the angular velocity. θ_1, θ_2, θ_3 are the rotation angles of OB, OA, OE respectively. For the sake of 3D analysis, the local coordinate system is established whose x-axis is perpendicular to the paper outwards with a varying origin along the center line of the curved cone. l is the value of y which is determined by the location where the cross-section of curved cone is intersected with tunnel face as the rotation angle ranges from θ_1 to θ_2. R is the radius of each cross-section of curved cone.

As shown in Fig. 2, the two logspiral curves, i.e. AE and BE, are respectively written as

$$r_1(\theta) = r_0' e^{(\theta-\theta_2)\tan\varphi} \tag{7}$$

$$r_2(\theta) = r_0 e^{-(\theta-\theta_1)\tan\varphi} \tag{8}$$

where θ is a variable denoting the rotation angle; r_0 and r'_0 are presented as follows.

$$r_0' = OA = \frac{d\sin\theta_1}{\sin(\theta_2-\theta_1)} \tag{9}$$

$$r_0 = OB = \frac{d\sin\theta_2}{\sin(\theta_2-\theta_1)} \tag{10}$$

and

$$\theta_3 = \frac{1}{2}\left[(\theta_1+\theta_2) - \frac{\ln(\sin\theta_1/\sin\theta_2)}{\tan\varphi}\right] \tag{11}$$

Provided that rm is the distance measured from the center of rotation O to the center line of curved cone, both of r_m and R can be expressed as functions of θ, namely

$$r_m = \frac{(r_1+r_2)}{2} = r_0 f_1(\theta) \tag{12}$$

$$R = \frac{(r_2-r_1)}{2} = r_0 f_2(\theta) \tag{13}$$

where the expressions of $f_1(\theta)$, $f_2(\theta)$ can be seen in Appendix.

To respect the upper bound theorem, the deterministic model is established by equating the rate of external work to

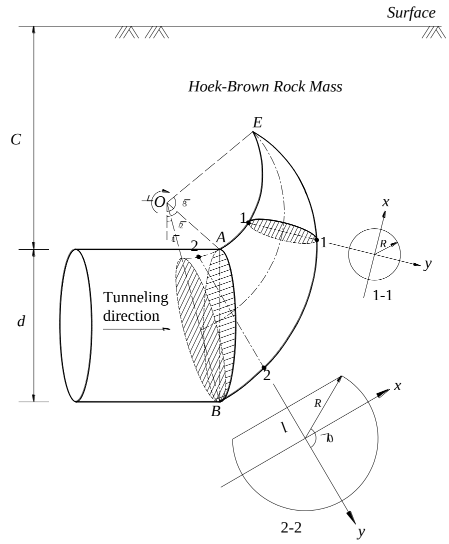

Fig. 2 Graphical representation of 3D tunnel face failure

the rate of the energy dissipation in any kinematically admissible velocity field. In combination with Hoek-Brown criterion, the work rate done by self-weight of rock mass P_γ is calculated with help of triple integral.

$$\begin{aligned} P_\gamma &= \int_{\theta_1}^{\theta_2}\int_{l}^{R}\int_0^{\sqrt{R^2-y^2}} 2\omega\gamma(r_m+y)^2\sin\theta\,dxdyd\theta \\ &+\int_{\theta_2}^{\theta_3}\int_{-R}^{R}\int_0^{\sqrt{R^2-y^2}} 2\omega\gamma(r_m+y)^2\sin\theta\,dxdyd\theta \\ &= \omega\gamma r_0^4[g_{11}(\theta_1,\theta_2)+g_{12}(\theta_2,\theta_3)] \end{aligned} \tag{14}$$

where γ=unit weight of rock mass, $l=r_0f_3(\theta)$ and the expressions of $g_{11}(\theta_1, \theta_2)$, $g_{12}(\theta_2,\theta_3)$, $f_3(\theta)$ are presented in Appendix.

Another part of external work rate done by support pressure PT can be expressed as

$$\begin{aligned} P_T &= \sigma_T\int_{\theta_1}^{\theta_2}\int_0^{\sqrt{R^2-l^2}} 2\omega(r_m+l)^2\cot\theta\,dxd\theta \\ &= \omega\sigma_T r_0^3 g_2(\theta_1,\theta_2) \end{aligned} \tag{15}$$

where σ_T is the uniform support pressure applied on tunnel face and $g_2(\theta_1, \theta_2)$ can be seen in Appendix.

For the curved cone, the work rate of energy dissipation PD is only produced along the sliding surface. By means of surface integral, it can be calculated as follows.

$$\begin{aligned} P_D &= 2\int_{\theta_1}^{\theta_2}\int_0^{\alpha_0}\omega c_t R(r_m+R\cos\alpha)^2 d\alpha d\theta \\ &+2\int_{\theta_2}^{\theta_3}\int_0^{\pi}\omega c_t R(r_m+R\cos\alpha)^2 d\alpha d\theta \\ &= \omega r_0^3[g_{31}(\theta_1,\theta_2)+g_{32}(\theta_2,\theta_3)] \end{aligned} \tag{16}$$

where $\alpha_0=\arccos(f_3/f_2)$ and the expressions of $g_{31}(\theta_1, \theta_2)$, $g_{32}(\theta_2, \theta_3)$ can be seen in Appendix.

Hence, the critical support pressure can be calculated as

$$\sigma_T = \frac{\gamma d\sin\theta_2[g_{11}+g_{12}]}{g_2\sin(\theta_2-\theta_1)} - \frac{[g_{31}+g_{32}]}{g_2} \tag{17}$$

For a tunnel excavated in Hoek-Brown rock mass, the inherent nonlinearity of rock mass is an important factor that affects the face stability. With resort to the generalized tangential technique, σT is optimized with the objective function of Eq. (6) and Eq. (17). The constraint conditions are given as follows.

$$s.t.\begin{cases} 0<\theta_1<\theta_2<\dfrac{\pi}{2} \\ \theta_2<\theta_3<\pi \\ 0<\varphi_t<\dfrac{\pi}{2} \end{cases} \tag{18}$$

3. Probabilistic model based on Kriging and MC

3.1 Kriging theory

This part is devoted to a short review of Kriging theory which states that the limit state function G(x) can be expressed as a regression model and a stochastic process (Echard *et al*. 2011, Gaspar *et al*. 2014).

$$G(\boldsymbol{x})=F(\boldsymbol{x})+\varepsilon(\boldsymbol{x}) \tag{19}$$

where x is the input vector; $F(x)$ is the trend function obtained by regression analysis; $\varepsilon(x)$ is the random error function representing the prediction error. The trend function is typically written as a low-order polynomial function as described in Eq. (20).

$$\begin{cases} F(\boldsymbol{x})=\beta_0 & \text{constant} \\ F(\boldsymbol{x})=\beta_0+\sum_{i=1}^{k}x_i\beta_i & \text{linear} \\ F(\boldsymbol{x})=\beta_0+\sum_{i=1}^{k}x_i\beta_i+\sum_{i=1}^{k}\sum_{j=1}^{k}x_ix_j\beta_{ij} & \text{second-order} \end{cases} \tag{20}$$

where k denotes the dimension of x and β=[β_0, β_1,…, β_k,…, β_{11}, β_{12},…β_{kk}]T denotes the vector of regression coefficients. The case of a constant trend function is known as "ordinary Kriging" which is most widely adopted and often suffices for high prediction accuracy. So the ordinary Kriging is adopted in this paper. It can be expected that the trend function can give a good prediction for the untried points that are close to the ones belonging to sampling points, but not for the distant ones. So it is inferred that the error function is spatially correlated. In Kriging theory, $\varepsilon(x)$ is considered as a stationary Gaussian process with the mean and the covariance between two points x and y as follows

$$\begin{cases} E(\varepsilon(\boldsymbol{x}))=0 \\ COV(\varepsilon(\boldsymbol{x}),\varepsilon(\boldsymbol{y}))=\sigma_\varepsilon^2R_\lambda(\boldsymbol{x},\boldsymbol{y}) \end{cases} \tag{21}$$

where σ^2_ε refers to the process variance and R_λ is the correlation function with undetermined parameters λ=[λ1, λ2,…λk]T. The Gaussian correlation function is most commonly used in literature as it is relatively smooth, infinitely differentiable and often numerically more stable which can be expressed as

$$R_\lambda(\boldsymbol{x},\boldsymbol{y})=\prod_{i=1}^{k}\exp\left[-\lambda_i(x_i-y_i)^2\right] \tag{22}$$

The parameter λ_i accounts for the correlation between $\varepsilon(x)$ and $\varepsilon(y)$ along the i-th random variable. An anisotropic correlation function with different λ_i for each random variable is preferred in the following studies to provide better flexibility in approaching the response surface.
Considering u sampling points [x_1, x_2,…,xu]T, the actual response Y=[Y_1, Y_2,…,Yu]T can be obtained by running $G(x)$ for each sampling point. So the scalars β_0 and σ^2_ε are estimated as follows.

$$\hat{\beta}_0=(\mathbf{1}^T\boldsymbol{R}^{-1}\mathbf{1})^{-1}\mathbf{1}^T\boldsymbol{R}^{-1}\boldsymbol{Y} \tag{23}$$

$$\hat{\sigma}_\varepsilon^2=\frac{1}{u}(\boldsymbol{Y}-\beta_0\mathbf{1})^T\boldsymbol{R}^{-1}(\boldsymbol{Y}-\beta_0\mathbf{1}) \tag{24}$$

where 1 represents the u dimensional column vector which is filled with 1 and R is the matrix of correlation and expressed as

$$\boldsymbol{R}=\begin{bmatrix} R_\lambda(\boldsymbol{x}^1,\boldsymbol{x}^1) & R_\lambda(\boldsymbol{x}^1,\boldsymbol{x}^2) & \cdots & R_\lambda(\boldsymbol{x}^1,\boldsymbol{x}^u) \\ R_\lambda(\boldsymbol{x}^2,\boldsymbol{x}^1) & R_\lambda(\boldsymbol{x}^2,\boldsymbol{x}^2) & \cdots & R_\lambda(\boldsymbol{x}^2,\boldsymbol{x}^u) \\ \cdots & \cdots & \cdots & \cdots \\ R_\lambda(\boldsymbol{x}^u,\boldsymbol{x}^1) & R_\lambda(\boldsymbol{x}^u,\boldsymbol{x}^2) & \cdots & R_\lambda(\boldsymbol{x}^u,\boldsymbol{x}^u) \end{bmatrix} \tag{25}$$

An indispensable precondition to obtain the estimations of β_0 and σ^2_ε is to calculate the value of λ by means of maximum likelihood estimation under the following objective function.

$$\hat{\boldsymbol{\lambda}}=\arg\min_\lambda(\det\boldsymbol{R})^{1/u}\hat{\sigma}_\varepsilon^2 \tag{26}$$

The best unbiased prediction $\hat{G}(x)$ at an untried point x can be written as

$$\hat{G}(\boldsymbol{x})=\beta_0+\boldsymbol{r}(\boldsymbol{x})^T\boldsymbol{R}^{-1}(\boldsymbol{Y}-\beta_0\mathbf{1}) \tag{27}$$

where $r(x)$=[$R_\lambda(x, x_1)$, $R\lambda(x, x_2)$,…, $R_\lambda(x, x_u)$]T.

The DACE provides an easily computable analytical function to evaluate the uncertainty of local prediction for untried points. The analytical function denoting the minimum of mean squared error (MSE) between $\hat{G}(x)$ and $G(x)$ is presented as

$$\sigma_{\hat{G}}^2(\boldsymbol{x})=\sigma_\varepsilon^2(1+f(\boldsymbol{x})^T(\mathbf{1}^T\boldsymbol{R}^{-1}\mathbf{1})^{-1}f(\boldsymbol{x})-\boldsymbol{r}(\boldsymbol{x})^T\boldsymbol{R}^{-1}\boldsymbol{r}(\boldsymbol{x})) \tag{28}$$

where $f(x)=1^TR^{-1}r(x)^{-1}$.

3.2 Algorithm of the probabilistic model

A probabilistic model for tunnel face stability is established combining Kriging and MC. Its basic idea is to construct a Kriging approximation model as a surrogate to classify a Monte Carlo population of N points without evaluating N times the actual limit state function. The proposed model can greatly reduce the computational time and costs without sacrificing the estimation accuracy of failure probability. To investigate the nonlinearity of

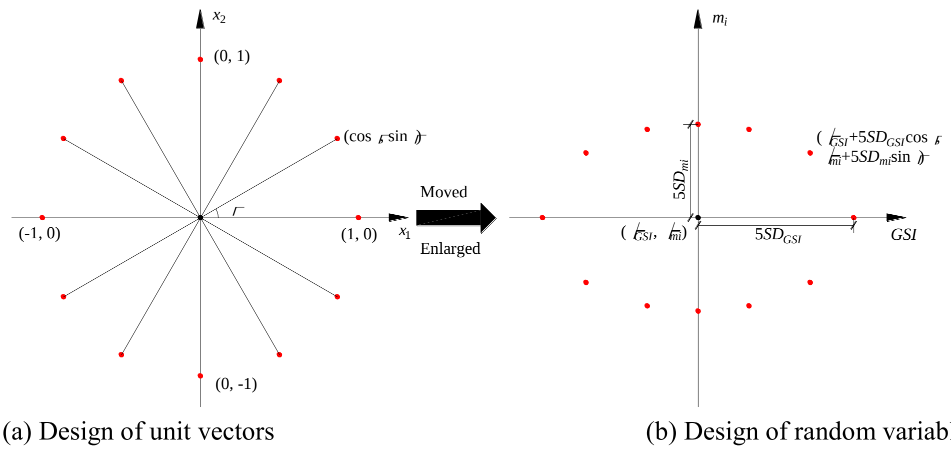

Fig. 3 Subdivision scheme of the uniform design

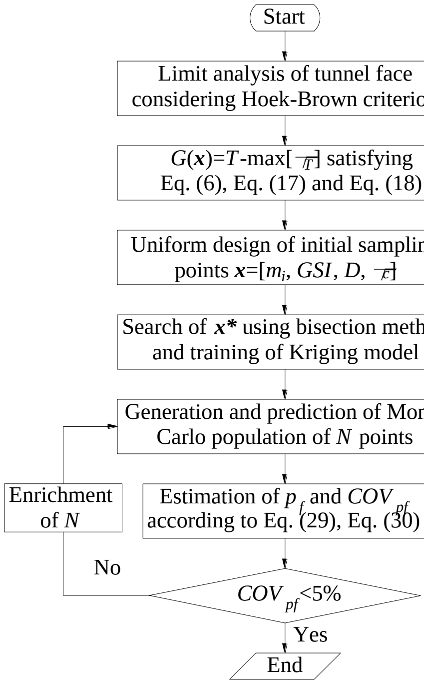

Fig. 4 Flow chart of the proposed probabilistic model

Table 1 The uniform table for probabilistic stability analysis of tunnel face

No.	m_i	GSI	D	σ_c
1	0	0	0	0
2	1	1	0	0
3	1	0	1	0
4	0	1	0	1
5	0	0	1	1

surrounding rock mass, the Hoek-Brown parameters mi, GSI, D and σ_c are treated as random variables and uniformly chosen to train the Kriging model. Fig. 4 presents the flow chart of the proposed probabilistic model where T denotes the support pressure against tunnel face, and it is based on the following steps:

(1) Uniform design of initial sampling points

The probabilistic stability analysis of tunnel face is started with constructing a Kriging model. It is an essential step to design a set of initial sampling points that are uniformly distributed in the space of random variables. In this contribution, the uniform design is obtained according to the uniform table as shown in Table 1. Each column represents a random variable and each row represents a combination of all random variables, namely a sampling point. It is inspired by the orthogonal table with two factors and two levels, where “0” represents the mean value and “1” represents an offset along the direction of each random variable. The offset takes 5 times the standard deviations of random variables to ensure that there are always several points on the opposite side of the mean-value point with respect to the limit state function. Fig. 3 presents a subdivision scheme of the uniform design to enrich the initial sampling points which actually contributes a lot to improvement of prediction accuracy of Kriging model. On the plane determined by each two random variables, the sampling points are selected for each fan-shaped area with a vertex of η (η=2π/q, q=1, 2, 3,…) which can be achieved by designing a set of unit vectors firstly (see Fig. 3(a)). Then the unit vectors are moved to the mean-value point and enlarged by the offset along each axial direction (see Fig. 3(b)). The subdivision scheme is performed for all the lines from the second to the fifth in Table 1.

(2) Approximation to limit state surface with bisection search

As a metamodel-based MC, the role of Kriging model is equivalent to a classifier. So only the sign (positive or negative) of the response instead of the exact value contributes to the estimation accuracy of failure probability. From this perspective, the most efficient way to improve the sign prediction of Kriging model is sampling as closely to the limit state surface as possible where the points have the highest probability to be mistakenly classified. To meet this requirement, the bisection method is adopted to search the points that are distributed on limit state surface. The mean-value point is set as one boundary for each bisection search and the initial sampling points whose responses have the opposite sign of the response at mean-value point are set as the other boundaries. The bisection searches are conducted and terminated with $G(x^*)$=0. Not surprisingly, x^* are the required points for Kriging model training.

(3) Estimation of failure probability

The Monte Carlo population of N points is generated according to the statistical properties of random variables. The trained Kriging model is used to predict the responses with small number of calls to actual limit state function. The responses that are less than 0 are counted as the number of occurrences of face failure which is labeled with N_f. The failure probability pf and its coefficient of variation COV_{pf} are estimated by Eq. (29) and Eq. (30) respectively.

$$p_f = \frac{N_f}{N} \tag{29}$$

$$COV_{p_f} = \sqrt{\frac{1-p_f}{Np_f}} \tag{30}$$

(4) End of the algorithm

COVpf is considered as an indicator of whether the size of Monte Carlo population N is large enough to give an acceptable estimation of failure probability. Traditionally, COVpf <5% means that the algorithm of the proposed approach can be terminated with a satisfying final result, otherwise the algorithm turns back to step 3 with a larger N.

4. Reliability analysis

4.1 Influence of uncertainty level

The proposed probabilistic model is used to assess the face stability under the influence of different uncertainty levels of random variables. Three probabilistic scenarios with different COVs of Hoek-Brown parameters are investigated as shown in Table 2. The other parameters in Fig. 2 is set as follows: C=30 m, d=10 m, γ=21 kN/m^3.

Based on the neutral scenario, Fig. 5 presents the normalized pf, which represents the rate of pf obtained by the proposed approach to that by direct MC, and number of calls to limit state function Ncall with the variation of n when T=50 kPa. It shows that the increase of n contributes to a high prediction accuracy of proposed approach. Meanwhile, it significantly reduces the computational efficiency due to the increase of initial sampling points. The normalized pf converges around n=12, which just ensures accurate estimation of failure probability with less costs in model training. So it is recommended that n is set to 12 in the following calculation.

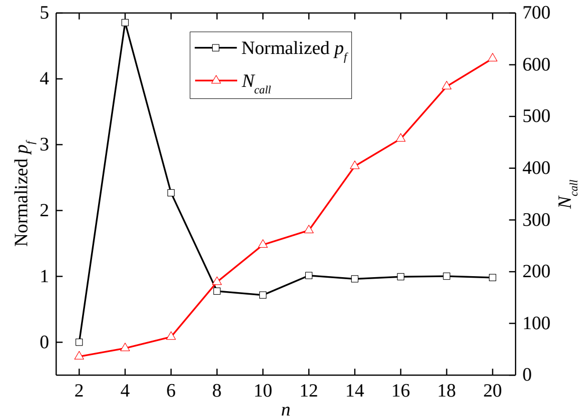

Fig. 5 The normalized pf and Ncall with the variation of n when T=50 kPa

Table 2 Statistical properties of Hoek-Brown parameters

Hoek-Brown parameter	Mean value (μ)	Coefficient of variation (COV)			Distribution type
		Optimistic scenario	Neutral scenario	Pessimistic scenario	
m_i	10	0.08	0.12	0.16	Normal
GSI	20	0.09	0.13	0.17	Normal
D	0.5	0.07	0.10	0.13	Normal
σ_c	1MPa	0.13	0.18	0.23	Normal

Table 3 presents the estimation of failure probability with different support pressures applied on tunnel face. The direct MC is performed for each case to validate the proposed probabilistic model except the ones that require more than five million trials. It is worth noting that the offset of uniform design should be reasonably adjusted for cases with high uncertainty level or extremely low failure probability to avoid generation of negative values or absence of available initial sampling points. As shown in Table 3, the failure probability estimated by proposed approach is very close to that given by direct MC for each case. The difference is about 5% or less. Ncall is listed to highlight the superior performance of proposed approach in improving computational efficiency. Compared with direct MC, Ncall is significantly reduced and it becomes more obvious when the failure probability is low. In addition, the uncertainty level has a distinct impact on failure probability especially when tunnel face is supported with greater pressure. The face stability is more significantly improved with enhancement of support pressure for the optimistic scenario. So it can concluded that more efficient reinforcements should be adopted to retain the face stability

Table 3 Failure probability with different support pressures

T/kPa	Scenario	Proposed approach			Direct MC			Difference (%)
		p_f	COV_{pf} (%)	N_{call}	p_f	COV_{pf} (%)	N_{call}	
30	Optimistic	3.82×10^{-2}	0.005	350	3.94×10^{-2}	4.33	1.3×10^{4}	3.05
	Neutral	1.09×10^{-1}	0.003	372	1.11×10^{-1}	4.01	5.0×10^{3}	1.63
	Pessimistic	1.89×10^{-1}	0.002	398	1.99×10^{-1}	4.01	2.5×10^{3}	5.21
40	Optimistic	1.10×10^{-3}	0.030	244	1.16×10^{-3}	4.96	3.5×10^{5}	5.17
	Neutral	1.99×10^{-2}	0.007	353	2.08×10^{-2}	4.02	3.0×10^{4}	4.33
	Pessimistic	6.33×10^{-2}	0.004	376	6.53×10^{-2}	4.23	8.0×10^{3}	3.01
50	Optimistic	3.84×10^{-5}	4.290	178	-	-	-	-
	Neutral	3.29×10^{-3}	0.017	280	3.35×10^{-3}	4.46	1.5×10^{5}	1.79
	Pessimistic	1.45×10^{-2}	0.008	328	1.52×10^{-2}	4.64	3.0×10^{4}	4.61
60	Optimistic	8.39×10^{-7}	4.370	123	-	-	-	-
	Neutral	6.35×10^{-4}	0.040	272	6.68×10^{-4}	4.78	7.0×10^{5}	4.94
	Pessimistic	7.37×10^{-3}	0.012	304	7.56×10^{-3}	4.68	6.0×10^{4}	2.49

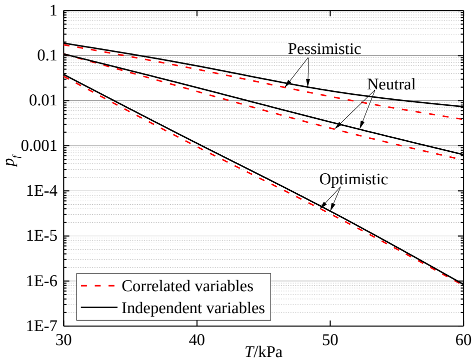

Fig. 6 Influence of correlated variables on failure probability

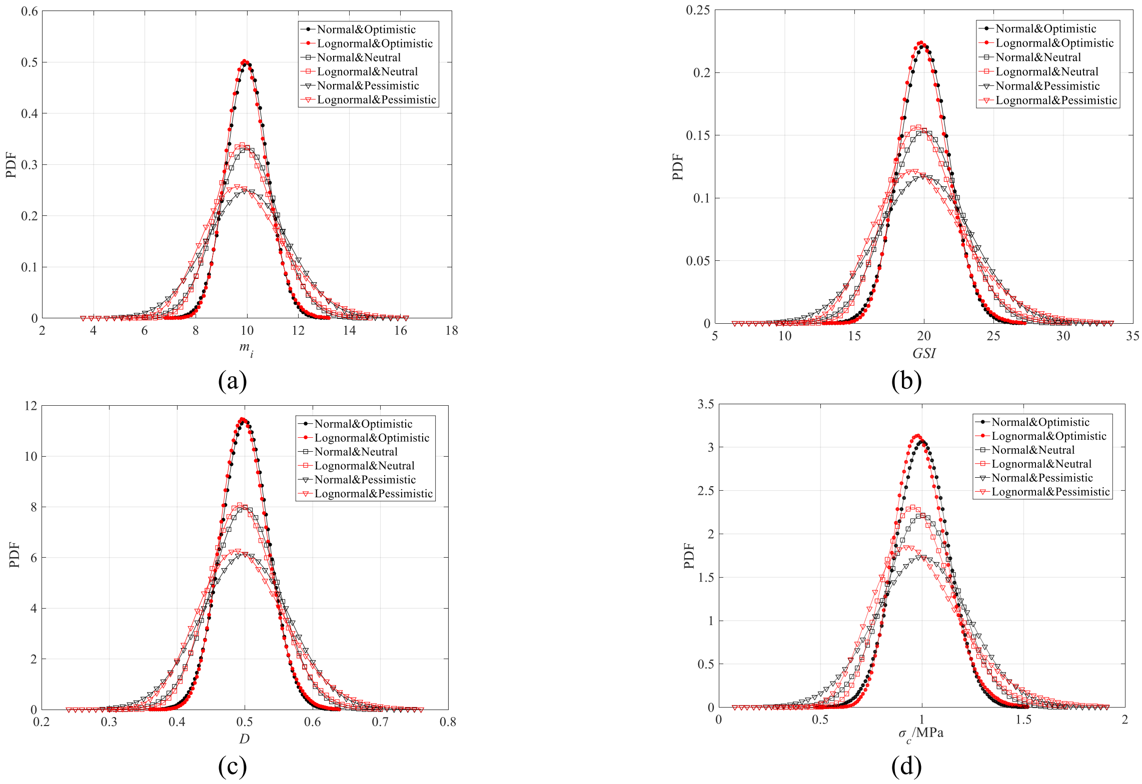

Fig. 7 PDF curves of random variables considering different distribution types

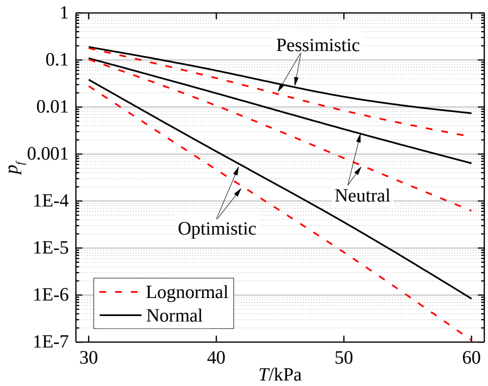

Fig. 8 Influence of distribution type on failure probability

for tunnels excavated in high uncertainty level rock mass.

4.2 Influence of correlated variables

Previous studies showed that the correlation between random variables has non-negligible influence on failure probability. Zhang *et al*. (2019) suggested that the nonlinear parameters were not independent from each other, but followed a certain correlation relationship. To figure out the influence of correlated Hoek-Brown parameters on failure probability, the following relationship is used in this contribution to define the correlation coefficients between mi, GSI, D and σc. The correlated data are generated using MATLAB. Fig. 6 presents the failure probability for each uncertainty level considering the influence of correlated variables. In comparison with independent variables, the correlated variables have slight influence on failure probability. The biggest difference occurs under the conditions of pessimistic scenario and T=60kPa, where pf is equal to 7.37×10-3 for independent variables and 3.84×10-3 for correlated ones. The increase of uncertainty level seems to make the influence of correlated variables more prominent.

4.3 Influence of distribution type

In terms of high uncertainty level of rock mass, the lognormal distribution is often adopted in lieu of normal distribution to exclude the physically meaningless negative values in numerical analysis. In order to investigate the influence of distribution type, the probabilistic stability analysis is performed based on lognormally distributed random variables in this section. Fig. 7 presents the curves of probability density function (PDF) of random variables with different distribution types. It is observed that the PDF curve of lognormally distributed variable shows a higher and earlier peak in comparison with normally distributed one. This phenomenon is intensified when a higher uncertainty level is considered. For the optimistic scenario, the PDF curves of two distribution types almost coincides with each other. However, obvious difference can be found between two curves for pessimistic scenario. As shown in Fig. 8, the failure probability derived from lognormally distributed variables is smaller than that from normally distributed ones. The difference becomes more obvious with a greater support pressure or a lower uncertainty level of random variables. It can be inferred that lognormal distribution may lead to a less conservative design in rock tunnel excavation, which permits a more economical design but may not be a safer one.

5. Conclusions

A model combing Kriging and Monte Carlo method is presented for probabilistic stability analysis of tunnel face in this paper. A novel uniform design is proposed to train the Kriging without requirement of iteratively adding new training points which can reduce much work in model training. The deterministic model is established based on upper bound theorem of limit analysis. With the help of generalized tangential technique, the Hoek-Brown failure criterion is introduced to account for the nonlinear behaviors of rock mass. The Hoek-Brown parameters mi, GSI, D, σ_c are treated as random variables. The following conclusions can be drawn:

• Failure probability of tunnel face is calculated by the proposed probabilistic model and direct MC respectively considering different uncertainty levels of random variables. It is shown that the failure probability estimated by the proposed approach is very close to that given by direct MC, while the former requires much less calls to actual limit state function. So it can be concluded that the proposed approach is an accurate and time-saving alternative for probabilistic stability analysis of tunnel face excavated in Hoek-Brown rock mass.

• The high uncertainty level of random variables leads to noticeable growth of failure probability. The face stability is improved significantly with the enhancement of support pressure for low uncertainty level, but not exactly for high uncertainty level case. It implies that more efficient reinforcements should be applied on tunnel face to retain its stability for poor condition rock mass.

• The influence of correlated variables is investigated based on a given matrix of correlation coefficients of mi, GSI, D, σ_c. Results show that the correlated variables have slight influence of failure probability. The increase of uncertainty level makes the influence of correlated variables more prominent.

• Lognormal distribution is employed to perform probabilistic analysis of tunnel face. Comparisons show that the PDF curve of lognormally distributed variable is taller and leans slightly forward. The lognormally distributed variables tend to given a positive estimation of failure probability. This tendency is intensified when a greater support pressure or a lower uncertainty level of random variables is considered.

In summary, the proposed probabilistic model is capable of handling stability problem of tunnel face excavated in spatially random Hoek-Brown rock mass. The uncertainty level, correlation relationship and distribution type of random variables have different impacts on failure probability, which should be considered carefully in engineering design.

Acknowledgments

The preparation of the paper has received financial supports from National Natural Science Foundation (51378510). The financial supports are greatly appreciated.

References

Aminpour, M.M., Maleki, M. and Ghanbari, A. (2017), "Investigation of the effect of surcharge on behavior of soil slopes", *Geomech. Eng.*, **13**(4), 653-669. https://doi.org/10.12989/gae.2017.13.4.653.

Ausilion, E. and Zimmaro, P. (2017), "Displacement-based seismic design of a shallow strip footing positioned near the edge of a rock slope", *Int. J. Rock Mech. Min. Sci.*, **76**, 68-77. https://doi.org/10.1016/j.ijrmms.2015.02.010.

Echard, B., Gayton, N. and Lemaire, M. (2011), "AK-MCS: An active learning reliability method combining Kriging and Monte Carlo simulation", *Struct. Safety*, **33**(2), 145-154. https://doi.org/10.1016/j.strusafe.2011.01.002.

Gaspar, B., Teixeira, A.P. and Soares, C.G. (2014), "Assessment of the efficiency of Kriging surrogate models for structural reliability analysis", *Prob. Eng. Mech.*, **37**, 24-34. https://doi.org/10.1016/j.probengmech.2014.03.011.

Hoek, E., Carranza-Torres, C. and Corkum, B. (2002), "Hoek-Brown failure criterion-2002 edition", *Proceedings of the 5th North American Rock Mechanics Symposium and the 17th Tunnelling Association of Canada Conference*, Toronto, Canada, July.

Jiang, Y., Luo, J., Liao, G., Zhao, Y. and Zhang, J. (2015), "An efficient method for generation of uniform support vector and its application in structural failure function fitting", *Struct. Safety*, **54**, 1-9. https://doi.org/10.1016/j.strusafe.2014.12.004.

Li, T.Z. and Yang, X.L. (2019b), "Face stability analysis of rock tunnels under water table using Hoek-Brown failure criterion", *Geomech. Eng.*, **18**(3), 235-245. https://doi.org/10.12989/gae.2019.18.3.235.

Li, T.Z., and Yang, X.L. (2019a), "3D rotational failure mechanism of tunnel face in weathered and saturated Hoek-Brown rock masses", *KSCE J. Civ. Eng.*, **23**(6), 2723-2732. https://doi.org/10.1007/s12205-019-1048-4.

Li, Y.X. and Yang, X.L. (2019c), "Soil-slope stability considering effect of soil-strength nonlinearity", *Int. J. Geomech.*, **19**(3), 04018201. https://doi.org/10.1061/(ASCE)GM.1943-5622.0001355.

Li, Y.X. and Yang, X.L. (2019d), "Seismic displacement of 3D slope reinforced by piles with nonlinear failure criterion", *Int. J. Geomech.*, **19**(6), 04019042. https://doi.org/10.1061/(ASCE)GM.1943-5622.0001411.

Li, Z.W. and Yang, X.L. (2019e), "Active earth pressure from unsaturated soils with different water levels", *Int. J. Geomech.*, **19**(7), 06019013. https://doi.org/10.1061/(ASCE)GM.1943-5622.0001471.

Li, Z.W. and Yang, X.L. (2019f), "Kinematical analysis of active earth pressure considering tension crack, pore-water pressure and soil nonlinearity", *KSCE J. Civ. Eng.*, **23**(1), 56-62. https://doi.org/10.1007/s12205-018-1098-z.

Michalowski, R.L. and Drescher, A. (2009), "Three-dimensional stability of slopes and excavations", *Géotechnique*, **59**(10), 839-850.

Miro, S., König, M., Hartmann, D. and Schanzb, T. (2015), "A probabilistic analysis of subsoil parameters uncertainty impacts on tunnel-induced ground movements with a back-analysis study", *Comput. Geotech.*, **68**, 38-53. https://doi.org/10.1016/j.compgeo.2015.03.012.

Nian, T.K., Liu, B., Han, J. and Huang, R.Q. (2014), "Effect of seismic acceleration directions on dynamic earth pressures in retaining structures", *Geomech. Eng.*, **7**(3), 263-277. http://dx.doi.org/10.12989/gae.2014.7.3.263.

Pan, Q. and Dias, D. (2017), "An efficient reliability method combining adaptive support vector machine and Monte Carlo simulation", *Struct. Safety*, **67**, 85-95. https://doi.org/10.1016/j.strusafe.2017.04.006.

Paternesi, A., Schweiger, H.F. and Scarpelli, G. (2017), "Numerical analyses of stability and deformation behavior of reinforced and unreinforced tunnel faces", *Comput. Geotech.*, **88**, 256-266. https://doi.org/10.1016/j.compgeo.2017.04.002.

Qin, C.B. and Chian, S.C. (2017), "2D and 3D stability analysis of tunnel roof collapse in stratified rock: A kinematic approach", *Int. J. Rock Mech. Min. Sci.*, **100**, 269-277. https://doi.org/10.1016/j.ijrmms.2017.10.027.

Serrano, A., Olalla, C. and Galindo, R.A. (2016), "Ultimate bearing capacity of an anisotropic discontinuous rock mass based on the modified Hoek-Brown criterion", *Int. J. Rock Mech. Min. Sci.*, **83**, 24-40. https://doi.org/10.1016/S0148-9062(97)00337-9.

Soomro, M.A., Ng, C.W.W., Liu, K. and Memona, N.A. (2017), "Pile responses to side-by-side twin tunnelling in stiff clay: Effects of different tunnel depths relative to pile", *Comput. Geotech.*, **84**, 101-116. https://doi.org/10.1016/j.compgeo.2016.11.011.

Xu, J.S. and Yang, X.L. (2019), "Seismic stability of 3D soil slope reinforced by geosynthetic with nonlinear failure criterion", *Soil Dyn. Earthq. Eng.*, **118**, 86-97. https://doi.org/10.1016/j.soildyn.2018.12.019.

Yang, X.L. and Chen, J.H. (2019b), "Factor of safety of geosynthetic-reinforced slope in unsaturated soils", *Int. J. Geomech.*, **19**(6), 04019041. https://doi.org/10.1061/(ASCE)GM.1943-5622.0001399.

Yang, X.L. and Zhang, S. (2019a), "Seismic active earth pressure for soils with tension cracks", *Int. J. Geomech.*, **19**(6), 06019009. https://doi.org/10.1061/(ASCE)GM.1943-5622.0001414.

Zhang, D.B., Jiang, Y. and Yang, X.L. (2019), "Estimation of 3D active earth pressure under nonlinear strength condition", *Geomech. Eng.*, **17**(6), 515-525. https://doi.org/10.12989/gae.2019.17.6.515.

Zhang, R. and Yang, X.L. (2019a), "Limit analysis of anchor trapdoor embedded in nonhomogeneous and nonlinear soils", *Int. J. Geomech.*, **19**(8), 04019089. https://doi.org/10.1061/(ASCE)GM.1943-5622.0001476.

Zhang, R. and Yang, X.L. (2019b), "New 3D failure analysis of water-filled karst cave beneath deep tunnel", *Geomech. Eng.*, **18**(1), 1-9. https://doi.org/10.12989/gae.2019.18.1.001.

Zou, J.F. and Xia, Z.Q. (2016), "Theoretical solutions for displacement and stress of a circular opening reinforced by grouted rock bolt", *Geomech. Eng.*, **11**(3), 439-455. https://doi.org/10.12989/gae.2016.11.3.439.

CC